This paper is available online at www.jbc.org

THE JOURNAL OF BIOLOGICAL CHEMISTRY VOL. 285, NO. 8, pp. 5117–5121, February 19, 2010

Identification of Thr^{29} as a Critical Phosphorylation Site That Activates the Human Proton Channel *Hvcn1* in Leukocytes*

Received for publication, November 5, 2009, and in revised form, December 15, 2009
Published, JBC Papers in Press, December 26, 2009, DOI 10.1074/jbc.C109.082727

Boris Musset[‡1], Melania Capasso[§1], Vladimir V. Cherny[‡], Deri Morgan[‡], Mandeep Bhamrah[§], Martin J. S. Dyer[§], and Thomas E. DeCoursey[‡2]

From the [‡]Department of Molecular Biophysics and Physiology, Rush University Medical Center, Chicago, Illinois 60612 and the [§]Toxicology Unit, Medical Research Council (MRC), University of Leicester, Leicester LE1 9HN, United Kingdom

Voltage-gated proton channels and NADPH oxidase function cooperatively in phagocytes during the respiratory burst, when reactive oxygen species are produced to kill microbial invaders. Agents that activate NADPH oxidase also enhance proton channel gating profoundly, facilitating its roles in charge compensation and pH_i regulation. The "enhanced gating mode" appears to reflect protein kinase C (PKC) phosphorylation. Here we examine two candidates for PKC-δ phosphorylation sites in the human voltage-gated proton channel, H_V1 (*Hvcn1*), Thr^{29} and Ser^{97}, both in the intracellular N terminus. Channel phosphorylation was reduced in single mutants S97A or T29A, and further in the double mutant T29A/S97A, by an *in vitro* kinase assay with PKC-δ. Enhanced gating was evaluated by expressing wild-type (WT) or mutant H_V1 channels in LK35.2 cells, a B cell hybridoma. Stimulation by phorbol myristate acetate enhanced WT channel gating, and this effect was reversed by treatment with the PKC inhibitor GF109203X. The single mutant T29A or double mutant T29A/S97A failed to respond to phorbol myristate acetate or GF109203X. In contrast, the S97A mutant responded like cells transfected with WT H_V1. We conclude that under these conditions, direct phosphorylation of the proton channel molecule at Thr^{29} is primarily responsible for the enhancement of proton channel gating. This phosphorylation is crucial to activation of the proton conductance during the respiratory burst in phagocytes.

Voltage-gated proton channels enable sustained superoxide anion (O_2^-) production by NADPH oxidase during the respiratory burst in phagocytes. NADPH oxidase generates O_2^- by transferring electrons from NADPH in the cytosol across the membrane to reduce extracellular or phagosomal O_2 to O_2^-. O_2^- is the precursor to other reactive oxygen species that contribute to killing microbial invaders. The consequences of NADPH oxidase activity, in particular decreased internal pH (pH_i) and membrane depolarization, are counteracted by H^+ efflux through open voltage-gated proton channels (1–6). The activities of NADPH oxidase and voltage-gated proton channels are coordinated in several ways. The depolarization and pH_i decrease resulting from NADPH oxidase activity both directly promote proton channel opening. In addition, interventions that activate NADPH oxidase profoundly enhance the gating properties of proton channels (3, 7). This "enhanced gating mode" consists of four changes in proton channel properties, each of which increases the likelihood of channel opening under any given set of conditions. The channels open faster (smaller activation time constant, τ_{act})[3] and close more slowly (larger deactivation time constant, τ_{tail}), display increased maximum proton conductance ($g_{H,max}$), and manifest a 40-mV hyperpolarizing shift of the entire proton conductance-voltage relationship (g_H-V). The enhanced gating mode improves the efficiency of NADPH oxidase by minimizing the depolarization required to open enough proton channels to fully compensate the electrical consequences of NADPH oxidase activity (*i.e.* the electron current) (5). Depolarization directly inhibits NADPH oxidase (4, 8).

The enhanced gating mode is induced by PMA, an activator of PKC, and is prevented and at least partially reversed by the PKC inhibitor GFX (9, 10). Although these results suggest regulation by PKC phosphorylation, they do not clarify whether the target of PKC is an accessory protein or the channel itself. This study identifies phosphorylation sites on the human proton channel molecule and determines their involvement in converting the proton channel to the enhanced gating mode. We find that a single residue, Thr^{29}, in the intracellular N-terminal domain appears to be responsible for inducing enhanced gating. Evidently, enhanced gating reflects a phosphorylated state of the proton channel and does not require accessory proteins.

EXPERIMENTAL PROCEDURES

Plasmids and Retroviral Infection—Myc-tagged *Hvcn1* was cloned by PCR in green fluorescent protein-bicistronic MigRI retroviral vector. *Hvcn1* T29A/S97A, T29A, T29D, S97A, and S97D mutants were generated by site-directed mutagenesis of wild-type *Hvcn1* sequence in MigRI vector using the Stratagene (La Jolla, CA) QuikChange technology. Sequences of primers used for mutagenesis are available upon request.

Lentiviral particles were prepared as follows. Phoenix α packaging cell line was transfected with empty vector con-

* This work was supported, in whole or in part, by National Institutes of Health Research Grant HL61437 through the NHLBI. This work was also supported by grants from Prof. Dr. Adolf Schmidtmann-Stiftung, Philip Morris USA Inc. and Philip Morris International, and the MRC, United Kingdom.

[1] Both authors contributed equally to this work.

[2] To whom correspondence should be addressed: Dept. of Molecular Biophysics and Physiology, Rush University Medical Center, 1750 West Harrison, Chicago, IL 60612. Tel.: 312-942-3267; Fax: 312-942-8711; E-mail: tdecours@rush.edu.

[3] The abbreviations used are: τ_{act}, activation time constant; τ_{tail}, deactivation (tail current) time constant; g_H, proton conductance; g_H-V, proton conductance-voltage relationship; I_H, steady-state proton current amplitude; CGD, chronic granulomatous disease; GFX, GF109203X; H_V1, the human *Hvcn1* voltage-gated proton channel gene product; PKC, protein kinase C; PMA, phorbol myristate acetate; WT, wild type; BES, 2-[bis(2-hydroxyethyl)amino]ethanesulfonic acid.

trol and *Hvcn1* MigRI plasmids by Ca^{2+} phosphate transfection. Viral supernatants were collected after 24, 36, and 48 h and frozen at −80 °C until use. LK35.2 cells were infected by spinoculation at 2300 rpm for 90 min in the presence of 4 μg/ml Polybrene (Sigma Aldrich, Dorset, UK) three times over a period of 2 days. At day 3, highly green fluorescent-protein-positive cells were sorted on a FACSVantage with CellQuest software (Becton Dickinson, Oxford, UK) and used for patch clamp studies.

In Vitro Kinase Assay—HEK-293 cells were transfected with Myc-tagged *Hvcn1*, *Hvcn1* T29A/S97A, *Hvcn1* T29A, and *Hvcn1* S97A MigRI constructs by Ca^{2+} phosphate. 24 h after transfection, cells were harvested and lysed (1% Triton X-100, 20 mM Hepes, 137 mM NaCl, 2.5 mM β-glycerophosphate, 1 mM Na_3O_4, 2 mM EDTA, protease inhibitor mixture (Sigma Aldrich)) prior to immunoprecipitation with anti-Myc antibody (Cell Signaling Technology) conjugated to protein G-Sepharose beads. Beads were then incubated in kinase assay buffer (20 mM Hepes, 1 mM EGTA, 0.4 mM EDTA, 5 mM $MgCl_2$, 0.1 mM $CaCl_2$, 0.05 mM dithiothreitol, 0.2 mg/ml phosphatidylinositol, 2.5 mM β-glycerophosphate, 1 μM PMA, 40 mM PKC-δ (Cell Signaling Technology), 10 μCi of [γ-^{32}P]ATP (GE Healthcare)) for 20 min at 30 °C, prior to being suspended in 2× Laemmli buffer. Four-fifths of samples were loaded on an SDS-PAGE that was then dried in a gel dryer prior to exposure to x-ray film; one-fifth of samples was loaded on a separate SDS-PAGE, transferred to nitrocellulose membrane, and immunoblotted with anti-Myc as loading control.

Electrophysiology—The recording and data analysis setups were as described previously (11). Pipettes were made from 7052 glass (Garner Glass Co., Claremont, CA). Seals were formed with Ringer's solution (in mM: 160 NaCl, 4.5 KCl, 2 $CaCl_2$, 1 $MgCl_2$, 5 Hepes, pH 7.4) in the bath, and the potential was zeroed after the pipette was in contact with the cell. For perforated patch recording, the pipette and bath solutions (~300 mosM) contained 130 mM tetramethylammonium methanesulfonate, 50 mM NH_4^+ in the form of 25 mM $(NH_4)_2SO_4$, 2 mM $MgCl_2$, 10 mM BES buffer, 1 mM EGTA and was titrated to pH 7.0 with tetramethylammonium hydroxide. The pipette solution included ~500 μg/ml solubilized amphotericin B (~45% purity; Sigma); the pipette tip was dipped in amphotericin-free solution. Experiments were done at 21 °C or at room temperature (20–25 °C).

The τ_{act} was obtained by fitting the rising current with a single exponential function, ignoring the initial sigmoid component. The steady-state H^+ current (I_H) was extrapolated using the fitted time constant. Deactivation was quantified by fitting tail currents with a single exponential to obtain the τ_{tail}. The values obtained for I_H along with reversal potential measured in each cell were used to calculate the g_H-V relationship. Shifts in the g_H-V relationship were assessed using plots like that in Fig. 2*D* and determining the shift by interpolation at the smallest reliable g_H values (where the voltage dependence is steepest). In some situations, the voltage at which time-dependent proton current was first detected, $V_{threshold}$, was used as a rough indicator of the position of the g_H-V relationship (12).

We routinely waited for stable recording conditions, added PMA, and later introduced GFX and considered the response genuine if PMA increased and GFX decreased the current. That the observed PMA responses were genuine was strongly corroborated by their reversal by GFX. Thus, although proton currents might increase due to improved access through the patch membrane or other spurious causes, it is unlikely that such increases would be reversed by GFX. Cells that were judged, based on access resistance, to have spontaneously entered whole-cell configuration were excluded from analysis. Responses to PMA or GFX are presented as ratios such that 1.0 means no response and a larger number means a larger response. Thus, for PMA responses, I_H(PMA)/I_H(control) and τ_{act}(control)/τ_{act}(PMA) are given. For GFX responses, I_H(PMA)/I_H(GFX) and τ_{act}(GFX)/τ_{act}(PMA) are given. Shifts in the g_H-V relationship were determined by interpolation of g_H values at voltages just above threshold.

RESULTS

In Vitro Kinase Assay for Phosphorylation—Fig. 1*A* shows the positions of two candidates for PKC phosphorylation sites tested here, Thr[29] and Ser[97]. These were identified by criteria determined by Fujii *et al.* (13). Both occur in the N terminus on intracellular regions of the human voltage-gated proton channel (H_V1) protein. It should be noted that because the structure of the proton channel is not known, the proximity of these sites to the membrane or to other parts of the channel is not established. Phosphorylation of these sites upon PMA stimulation was assessed in an *in vitro* kinase assay with recombinant PKC-δ. Fig. 1*B* shows that phosphorylation was reduced significantly when compared with WT H_V1 for either single mutant S97A or T29A. Phosphorylation was further reduced in the double mutant T29A/S97A, which supports the conclusion that both sites are phosphorylated by PKC-δ.

Electrophysiological Measurements of Enhanced Gating—Identifying sites that might contribute to enhanced gating requires an expression system in which expressed proton channels respond to PMA. Although proton channels in human neutrophils and eosinophils respond dramatically to PMA (7, 14), HEK-293 cells transfected with the proton channel, *Hvcn1*, do not respond (12). However, we found that when *Hvcn1* is expressed in the B lymphocytic cell line, LK35.2, the resulting proton current responds to PMA in a manner qualitatively like the response of human phagocytes (Fig. 2*F*). An advantage of the LK35.2 B lymphocytic line is that cells that were not transfected or transfected with empty vector had no detectable proton currents ($n = 8$), whereas LK35.2 cells transfected with *Hvcn1* expressed large proton currents (Fig. 2*A*). The experimental approach is illustrated in Fig. 2*F*. Test pulses were applied, and then PMA was introduced, after which the proton current amplitude I_H increased progressively over several minutes. On average, I_H increased 2.4-fold during test pulses (Table 1). After application of a voltage clamp family and measurement of the reversal potential, V_{rev}, test pulses were again applied. Then GFX was added to the bath, and the enhanced proton current was progressively reduced toward its amplitude before stimulation.

In each experimental condition, we applied families of depolarizing pulses, as illustrated in Fig. 2, *A–C*, to characterize the response in greater detail. Fig. 2*D* shows that PMA increased g_H

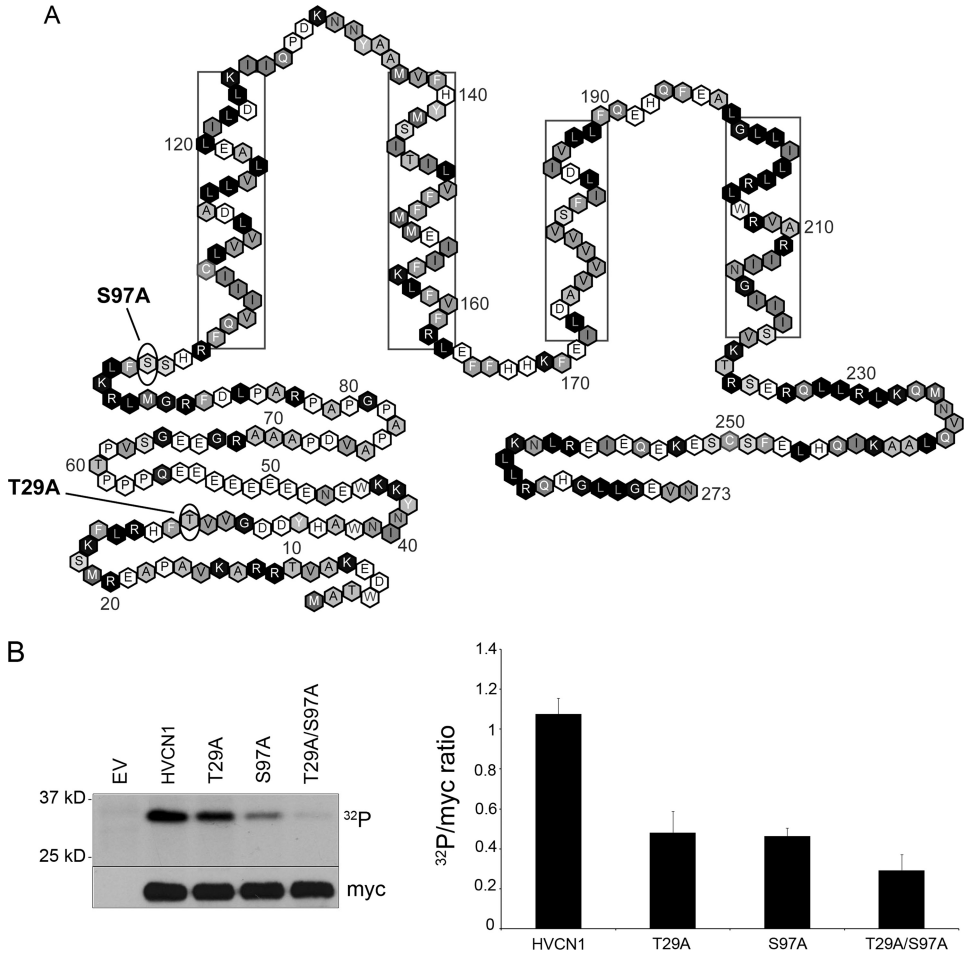

FIGURE 1. **Identification of candidate phosphorylation sites in the human proton channel.** *A*, location of the two putative PKC-δ phosphorylation sites in the sequence of H_V1. Both predicted PKC-δ sites are in the N terminus, with Ser[97] near the membrane boundary. *Boxed residues* indicate helical transmembrane regions (37). *B*, phosphorylation of H_V1 WT, T29A, S97A, and T29A/S97A mutants in the presence of recombinant PKC-δ and [γ-[32]P]ATP in an *in vitro* kinase assay. PKC-δ was activated with 1 μM PMA. The *myc immunoblot* indicates loading. *EV* indicates empty vector control. The graph on the right-hand side represents densitometric analysis of the [32]P band *versus* loading control of 3–4 separate experiments ($p < 0.05$ for each mutant *versus* WT by Student's *t* test). *Error bars* indicate S.E.

and shifted the g_H-V relationship negatively. The mean shift of the g_H-V relationship was −11 mV (Table 1). GFX reversed this shift substantially. The rate of channel opening increased after PMA stimulation; the time constant of H^+ current activation, τ_{act}, became twice faster. Fig. 2*E* shows that the proportional change in τ_{act} was similar at all voltages. GFX reversed the change in τ_{act} (Fig. 2*E*). The effects of PMA and GFX on proton channel parameters are summarized in Table 1. In contrast with the responses of proton currents in human phagocytes, there was little slowing of deactivation (τ_{tail}). The differences in the PMA responses of LK35.2 cells when compared with human neutrophils may reflect the lack of NADPH oxidase activity in LK35.2 cells (15) (see "Discussion").

Responses of Mutant Proton Channels—The two candidate phosphorylation sites were mutated to Ala individually (S97A and T29A) and together. We also studied mutants S97D and T29D designed as phosphorylation mimics. LK35.2 cells transfected with the double mutant proton channel (S97A/T29A) never responded detectably to PMA or GFX ($n = 15$). Similarly, no response was detected in the T29A (Fig. 2*G*) or T29D mutants, with the exception of a possible small response in 1 of 12 cells studied. However, the S97A and S97D mutants did respond (Table 1). Combined, these results strongly implicate Thr[29] as the key phosphorylation site on the human proton channel.

If Thr[29] is the primary phosphorylation site, then the designed phosphorylation mimic T29D might already appear "activated," in comparison with WT channels. In this scenario, the expectation would be that the threshold voltage, $V_{threshold}$, would be more negative than WT. Examination of $V_{threshold}$ for such an effect revealed that the WT channel was first distinctly activated at +2.1 ± 2.2 mV (mean ± S.E., $n = 17$). $V_{threshold}$ in T29D expressing cells was −0.7 ± 4.4 mV ($n = 7$), a small shift in the expected direction but not significantly different. The effects of PMA and GFX on individual cells are clearly evident because each cell serves as its own control. In contrast, detecting a small difference in properties between populations of unstimulated cells may not be feasible. Alternatively, phosphorylation mimics ($X \rightarrow$ Glu or $X \rightarrow$ Asp) are not always distinguishable from simple alanine mutants ($X \rightarrow$ Ala) (16).

The lack of response of Thr[29] mutants suggests that the entire phosphorylation response is ascribable to phosphorylation of Thr[29]. However, we compared the responses in Ser[97] mutants statistically to test the possibility that Ser[97] might contribute measurably to the response (Table 1). Although the enhancement of proton channel gating by PMA and its reversal by GFX tended to be larger in WT controls than in Ser[97] mutants, the difference failed to reach statistical significance for any parameter (whether S97A and S97D were compared with WT separately or together). However, the probability that all eight parameters would exhibit smaller responses in S97X than WT is <0.01. Thus, we cannot rule out that Ser[97] may play a minor role or affect other functions of the channel. However, it is clear that phosphorylation of Thr[29] is the major contributor to the enhanced gating of proton channels.

DISCUSSION

Voltage-gated proton channels are necessary for a normal phagocyte respiratory burst; NADPH oxidase activity by neutrophils, eosinophils, monocytes, macrophages, B lymphocytes and PLB-985 cells is greatly reduced when proton currents are inhibited by Zn^{2+} or other polyvalent metal cations (4, 9, 17–22) or when the proton channel is removed genetically (23–

25). Proton channels and NADPH oxidase are both activated during phagocytosis, but their interaction is complex, and the mechanism remains controversial (15). The idea that the proton channel is part of the NADPH oxidase complex (26) and is thus active *de facto* during NADPH oxidase activity (3) appears untenable in light of the demonstration of NADPH oxidase-generated electron current in phagocytes from *Hvcn1*-deficient mice (6). Another view is that these two molecules are activated independently but by similar pathways (10).

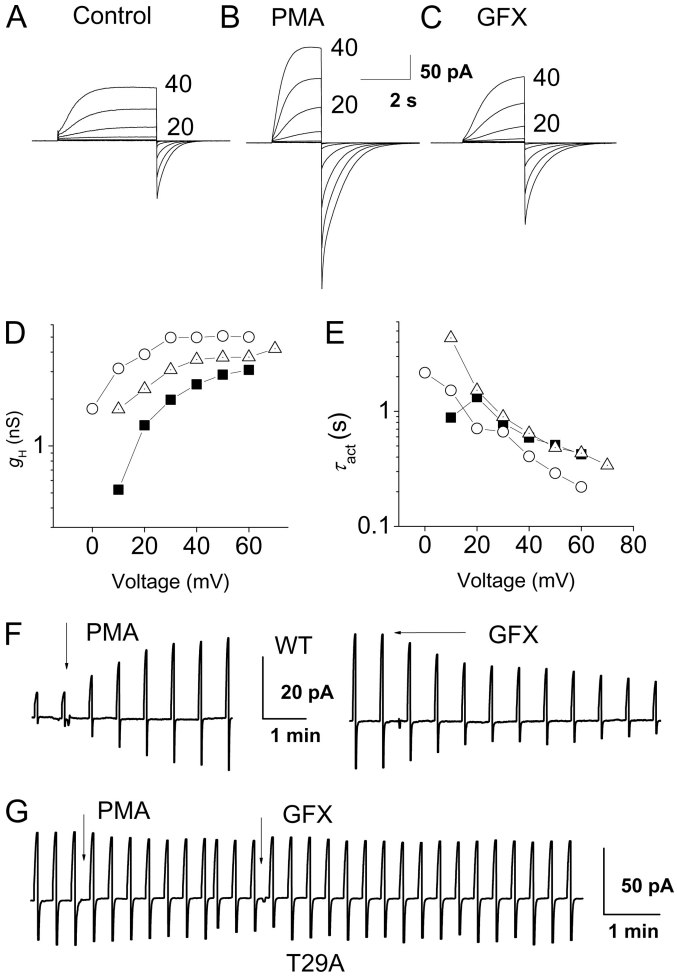

FIGURE 2. **Enhanced proton channel gating elicited by PMA and reversed by GFX in an LK35.2 cell.** *A–C*, families of proton currents during pulses in 10-mV increments up to +40 mV in an *Hvcn1*-transfected LK35.2 cell before (*A*) or after PMA stimulation (*B*) and after GFX (*C*). *D*, the steady-state g_H, calculated from the currents in *A* (■), *B* (○), and *C* (△) after fitting to a rising exponential, using reversal potentials measured in each solution. *E*, τ_{act} values in the same cell are faster after PMA, but the effect is reversed by GFX. *F*, time course of PMA and GFX responses in the cell in *A–E*, with test pulses to +10 mV repeated every 38 s from a holding potential of −40 mV. During the break in the time course, after the addition of PMA, the family of currents in *B* was recorded. *G*, proton currents during pulses to +20 mV repeated every 20 s from a holding potential of −40 mV in an LK35.2 cell transfected with the T29A mutant channel did not respond to PMA or GFX.

The suspicion that voltage-gated proton channels in leukocytes are activated by PKC phosphorylation (10, 27, 28) is strongly supported by the present results. Furthermore, our data indicate that the channel protein itself is phosphorylated. The *in vitro* kinase assay detected phosphorylation of both Ser[97] and Thr[29]. However, in our experimental system, Thr[29] appeared to be responsible for the entire measurable response of proton channels. T29A or T29D mutants did not respond to PMA, nor did the double mutant T29A/S97A. In contrast, S97A or S97D mutants did respond to PMA, although their response may have been slightly weaker than that of WT channels (Table 1). These results do not resolve the physiological significance of phosphorylation of Ser[97]. That Ser[97] was phosphorylated, yet S97A and S97D exhibited no deficit, is not without precedent. Many proteins have multiple phosphorylation sites of which only a fraction exert specific functional effects. For example, cardiac troponin T has four phosphorylation sites, of which only one exhibited functional defects upon mutation (16). Another protein with multiple phosphorylation sites is $p47^{phox}$, whose phosphorylation is an absolute prerequisite for NADPH oxidase assembly and function. Individual mutation of 10 phosphorylated serines revealed just one mutation, S379A, that abolished activation, five Ser → Ala mutations that inhibited activation by ~50%, and three that had no effect (29).

In future studies, we will attempt to identify the PKC isoform that phosphorylates the proton channel. By criteria determined by Fujii *et al.* (13), Thr[29] is a likely PKC-δ site, but ScanSite identifies Thr[29] as a possible target for cAMP-dependent protein kinase, PKC-μ, Akt kinase, or calmodulin kinase. Ser[97] is also identified by criteria determined by Fujii *et al.* (13) as a likely PKC-δ site, but ScanSite identifies Ser[97] as a possible target for PKC-α, PKC-β, or PKC-γ. PKC-δ appears to be important in responses of human phagocytes (9, 30–32) and murine B lymphocytes (33, 34).

Proton channels studied in perforated-patch conditions in human neutrophils, eosinophils, monocytes, and to a lesser extent, in basophils, respond dramatically to PMA (7, 12, 14, 35). In contrast, proton channels in other cells, such as rat alve-

TABLE 1

Effects of PMA and GFX on proton channel parameters (mean ± S.E. (*n*))

Relative values of proton channel parameters in each cell before (c = control) or after PMA stimulation and after GFX reversal are shown. All ratios are presented so that a larger number means a larger effect. The g_H-V relationship shift by PMA is relative to control, and GFX is relative to PMA (see "Experimental Procedures"). The T29A, T29D, and double mutant T29A/S97A did not respond. Significance by one-sample *t* test, *, $p < 0.05$, **, $p < 0.01$, compared with no effect (1.0 for ratios, 0 for g_H-V shift). None of the differences between WT and S97D or S97A are significant (Student's *t* test). For comparison, average parameter values from human neutrophils from CGD patients and normal subjects from a previous study (36) are given in columns 4 and 5, respectively.

	WT	S97A or S97D	CGD neutrophils	Neutrophils
I_H PMA/c	2.39* ± 0.51 (10)	1.42** ± 0.13 (12)	2.55	3.3
I_H PMA/GFX	2.19** ± 0.37 (12)	1.22 ± 0.11 (8)		
τ_{act} c/PMA	2.12 ± 0.53 (10)	1.62** ± 0.15 (12)	1.94	3.7
τ_{act} GFX/PMA	1.87** ± 0.22 (12)	1.51* ± 0.21 (8)		
τ_{tail} PMA/c	1.22 ± 0.11 (10)	1.13 ± 0.067 (12)	1.15	5.5
τ_{tail} PMA/GFX	1.54** ± 0.17 (13)	1.14 ± 0.06 (8)		
g_H-V shift PMA (mV)	−10.7** ± 1.9 (7)	−7.8** ± 1.6 (8)	−13.3	−38.8
g_H-V shift GFX (mV)	9.4** ± 1.6 (8)	6.7** ± 1.2 (7)		

olar epithelial cells (7) or HEK-293 or COS-7 cells transfected with H_V1 (12), do not respond at all. Hypothetical explanations for this variable response in different tissues include (*a*) different proton channel isoforms, (*b*) different signaling pathways, and (*c*) regulation of the channel by a separate molecule whose phosphorylation modulates proton channel behavior (15). Our results do not support the existence of a separate regulatory molecule (other than NADPH oxidase; see next paragraph).

Proton channels expressed in the B lymphocytic cell line LK35.2 were found to respond qualitatively like those in primary leukocytes, but the response was substantially less profound (Table 1). Each of the four main responses is weaker in LK35.2 cells than in neutrophils, but the most obvious differences are the lack of profound slowing of channel closing (τ_{tail}) and the smaller hyperpolarizing shift of the g_H-V relationship. The requirements for a full phagocyte-like proton channel response are unclear. Circumstantial evidence suggests that a crucial factor is the presence or absence of NADPH oxidase activity. Neutrophils from chronic granulomatous disease (CGD) patients lack functional NADPH oxidase and also exhibit a reduced PMA response with no slowing of τ_{tail} and only an ~10-mV hyperpolarization of the g_H-V relationship (36). The responses of proton channels in LK35.2 cells were essentially identical to the responses in CGD cells (Table 1) and in PLB-985 cells lacking $gp91^{phox}$ (36). We did not detect electron current in PMA-stimulated LK35.2 cells, consistent with low levels of NADPH oxidase activity (23). Human basophils also lack NADPH oxidase and exhibit PMA and GFX responses smaller than those of neutrophils or eosinophils and specifically lack a slowing of τ_{tail} (35). Thus, it is clear that a proton channel response is possible without NADPH oxidase, but the response differs in characteristic ways from that in cells with NADPH oxidase activity. The alternative postulate, that proton channels are preferentially phosphorylated by specific PKC isoforms that are more active in phagocytes, does not explain the meager response of CGD neutrophils (Table 1).

In summary, enhanced gating of H_V1 is primarily the result of phosphorylation at Thr^{29} by PKC. The magnitude and specific characteristics of the PMA response in LK35.2 cells closely resembled that in other cells lacking NADPH oxidase activity, suggesting that a crucial interaction between these molecules occurs in phagocytes. The identification of the location of the key phosphorylation site that activates phagocyte proton channels provides a rational target for modulation of innate immune responses.

REFERENCES

1. Henderson, L. M., Chappell, J. B., and Jones, O. T. (1987) *Biochem. J.* **246,** 325–329
2. DeCoursey, T. E., and Cherny, V. V. (1993) *Biophys. J.* **65,** 1590–1598
3. Bánfi, B., Schrenzel, J., Nüsse, O., Lew, D. P., Ligeti, E., Krause, K. H., and Demaurex, N. (1999) *J. Exp. Med.* **190,** 183–194
4. DeCoursey, T. E., Morgan, D., and Cherny, V. V. (2003) *Nature* **422,** 531–534
5. Murphy, R., and DeCoursey, T. E. (2006) *Biochim. Biophys. Acta* **1757,** 996–1011
6. Morgan, D., Capasso, M., Musset, B., Cherny, V. V., Ríos, E., Dyer, M. J., and DeCoursey, T. E. (2009) *Proc. Natl. Acad. Sci. U.S.A.* **106,** 18022–18027
7. DeCoursey, T. E., Cherny, V. V., Zhou, W., and Thomas, L. L. (2000) *Proc. Natl. Acad. Sci. U.S.A.* **97,** 6885–6889
8. Petheo, G. L., and Demaurex, N. (2005) *Biochem. J.* **388,** 485–491
9. Bankers-Fulbright, J. L., Kita, H., Gleich, G. J., and O'Grady, S. M. (2001) *J. Cell. Physiol.* **189,** 306–315
10. Morgan, D., Cherny, V. V., Finnegan, A., Bollinger, J., Gelb, M. H., and DeCoursey, T. E. (2007) *J. Physiol.* **579,** 327–344
11. Morgan, D., Cherny, V. V., Murphy, R., Xu, W., Thomas, L. L., and DeCoursey, T. E. (2003) *J. Physiol.* **550,** 447–458
12. Musset, B., Cherny, V. V., Morgan, D., Okamura, Y., Ramsey, I. S., Clapham, D. E., and DeCoursey, T. E. (2008) *J. Physiol.* **586,** 2477–2486
13. Fujii, K., Zhu, G., Liu, Y., Hallam, J., Chen, L., Herrero, J., and Shaw, S. (2004) *Proc. Natl. Acad. Sci. U.S.A.* **101,** 13744–13749
14. DeCoursey, T. E., Cherny, V. V., DeCoursey, A. G., Xu, W., and Thomas, L. L. (2001) *J. Physiol.* **535,** 767–781
15. Musset, B., Cherny, V. V., Morgan, D., and DeCoursey, T. E. (2009) *FEBS Lett.* **583,** 7–12
16. Sumandea, M. P., Pyle, W. G., Kobayashi, T., de Tombe, P. P., and Solaro, R. J. (2003) *J. Biol. Chem.* **278,** 35135–35144
17. Chvapil, M., Stankova, L., Bernhard, D. S., Weldy, P. L., Carlson, E. C., and Campbell, J. B. (1977) *Infect. Immun.* **16,** 367–373
18. Henderson, L. M., Chappell, J. B., and Jones, O. T. (1988) *Biochem. J.* **255,** 285–290
19. Simchowitz, L., Foy, M. A., and Cragoe, E. J., Jr. (1990) *J. Biol. Chem.* **265,** 13449–13456
20. Lowenthal, A., and Levy, R. (1999) *J. Biol. Chem.* **274,** 21603–21608
21. Femling, J. K., Cherny, V. V., Morgan, D., Rada, B., Davis, A. P., Czirják, G., Enyedi, P., England, S. K., Moreland, J. G., Ligeti, E., Nauseef, W. M., and DeCoursey, T. E. (2006) *J. Gen. Physiol.* **127,** 659–672
22. Musset, B., Cherny, V., and DeCoursey, T. E. (2009) *Biophys. J.* **96,** 667a–668a
23. Capasso, M., Bhamrah, M. K., Henley, T., Boyd, R. S., Langlais, C., Cain, K., Dinsdale, D., Pulford, K., Khan, M., Musset, B., Cherny, V. V., Morgan, D., Gascoyne, R. D., Vigorito, E., DeCoursey, T. E., MacLennan, I. C., and Dyer, M. J. (2010) *Nat. Immunol.*, in press
24. Ramsey, I. S., Ruchti, E., Kaczmarek, J. S., and Clapham, D. E. (2009) *Proc. Natl. Acad. Sci. U.S.A.* **106,** 7642–7647
25. Okochi, Y., Sasaki, M., Iwasaki, H., and Okamura, Y. (2009) *Biochem. Biophys. Res. Commun.* **382,** 274–279
26. Henderson, L. M., Banting, G., and Chappell, J. B. (1995) *J. Biol. Chem.* **270,** 5909–5916
27. Nanda, A., and Grinstein, S. (1991) *Proc. Natl. Acad. Sci. U.S.A.* **88,** 10816–10820
28. Kapus, A., Szászi, K., and Ligeti, E. (1992) *Biochem. J.* **281,** 697–701
29. El-Benna, J., Dang, P. M., Gougerot-Pocidalo, M. A., Marie, J. C., and Braut-Boucher, F. (2009) *Exp. Mol. Med.* **41,** 217–225
30. He, R., Nanamori, M., Sang, H., Yin, H., Dinauer, M. C., and Ye, R. D. (2004) *J. Immunol.* **173,** 7462–7470
31. Zhao, X., Xu, B., Bhattacharjee, A., Oldfield, C. M., Wientjes, F. B., Feldman, G. M., and Cathcart, M. K. (2005) *J. Leukoc. Biol.* **77,** 414–420
32. Cheng, N., He, R., Tian, J., Dinauer, M. C., and Ye, R. D. (2007) *J. Immunol.* **179,** 7720–7728
33. Mecklenbräuker, I., Saijo, K., Zheng, N. Y., Leitges, M., and Tarakhovsky, A. (2002) *Nature* **416,** 860–865
34. Miyamoto, A., Nakayama, K., Imaki, H., Hirose, S., Jiang, Y., Abe, M., Tsukiyama, T., Nagahama, H., Ohno, S., Hatakeyama, S., and Nakayama, K. I. (2002) *Nature.* **416,** 865–869
35. Musset, B., Morgan, D., Cherny, V. V., MacGlashan, D. W., Jr., Thomas, L. L., Ríos, E., and DeCoursey, T. E. (2008) *Proc. Natl. Acad. Sci. U.S.A.* **105,** 11020–11025
36. DeCoursey, T. E., Cherny, V. V., Morgan, D., Katz, B. Z., and Dinauer, M. C. (2001) *J. Biol. Chem.* **276,** 36063–36066
37. Ramsey, I. S., Moran, M. M., Chong, J. A., and Clapham, D. E. (2006) *Nature* **440,** 1213–1216